Supporting Information

A novel phosphorescent iridium(III) complex bearing donor-acceptor-type *o*−carboranylated ligand for endocellular hypoxia imaging

Xiang Li,[a] Yongheng Yin,[a] Pengli Gao,[b] Weijie Li,[a] Hong Yan,*[a] Changsheng Lu,*[a] and Qiang Zhao*[b]

[a] State Key Laboratory of Coordination Chemistry, School of Chemistry and Chemical Engineering, Nanjing University, Nanjing, Jiangsu 210023, China

[b] Key Laboratory for Organic Electronics and Information Displays & Institute of Advanced Materials, National Jiangsu Syngerstic Innovation Center for Adavanced Materials, Nanjing University of Posts and Telecommunications, Nanjing, Jiangsu 210023, China

CONTENTS

I. General methods

In this work, all the synthetic steps were carried out under an inert argon atmosphere using standard Schlenk line and glovebox techniques unless otherwise noted. Commercial reagents were used without any further purification after purchasing. Ether and toluene were distilled on sodium / benzophenone. Acetonitrile, dichloromethane, and methanol were distilled on CaH_2. All the solvents are freshly distilled. Dimeric $[(C\text{^}N)_2Ir(\mu\text{−}Cl)]_2$ complex,[S1] the precursors 5−bromo−2,2′−bipyridine (**a**),[S2] 5−*o*−carboranyl−2−bromopyridine,[S3] 6−bromo−*N*,*N*−diphenyl pyridin−3−amine (**b**),[S4] and *N*,*N*−diphenyl−6−(trimethylstannyl)pyridine−3−amine (**c**)[S2] were prepared by literature procedures. The intermediate compound $B_{10}H_{12}(Et_2S)_2$ was synthesized by a modified method according to literature reports.[S5] NMR spectra (^1H−, ^{13}C−, and ^{11}B−) were recorded on Bruker DRX−500 and DRX−400 at ambient temperature. Chemical shifts are reported relative to $CHCl_3$ / $CDCl_3$ (δ ^1H = 7.26 ppm, δ ^{13}C = 77.0 ppm), $(CH_3)_2CO$ / $(CD_3)_2CO$ (δ ^1H = 2.05 ppm, δ ^{13}C = 205.0 ppm) and external $Et_2O{\cdot}BF_3$ (δ ^{11}B = 0 ppm), respectively. EI−MS (Micromass GC−TOF (70 eV)) was used for all the ligands. ESI−MS (LCQ Fleet, Thermo Fisher Scientific) was used to detect ionic iridium complexes. UV−vis absorption spectra were recorded with Shimadzu UV−2550 spectrophotometers. PL spectra were recorded on a Hitachi F−4600 fluorescence spectrophotometer. PL lifetime measurements were performed by employing an Edinburgh FLS 920 spectrophotometer equipped with laser impulse fluorometer of picosecond time resolution. Absolute quantum yields were measured by using an integrating sphere. X−ray diffraction data were collected on a Bruker Smart CCD Apex DUO diffractometer with graphite monochromated Mo Kα radiation (λ = 0.71073 Å) using the ω−2θ scan mode.

II：Syntheses

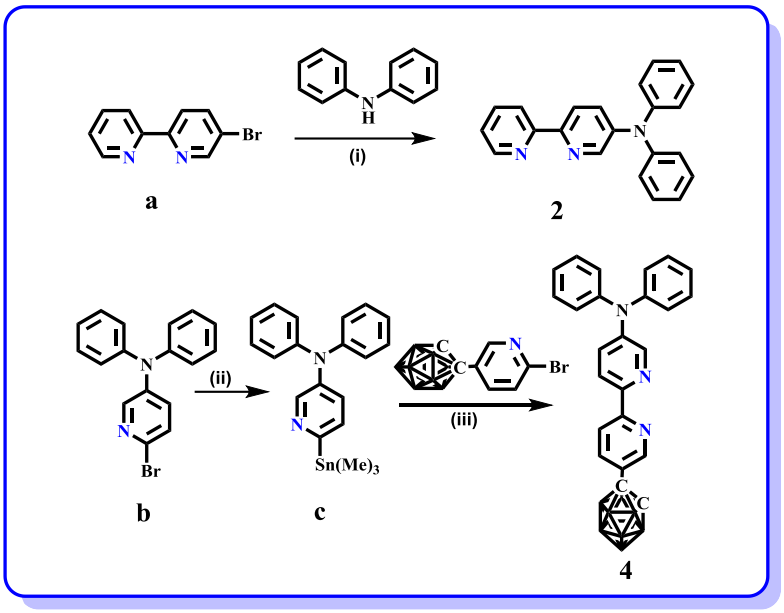

Scheme S1. Syntheses of the ancillary ligands: (i) $Pd_2(dba)_3$, BINAP, sodium−*tert*−butoxide, 130°C, toluene; (ii) *n*−BuLi, trimethylstannyl chloride, ether; (iii) $Pd(PPh_3)_4$, xylenes, refluxing for 24h.

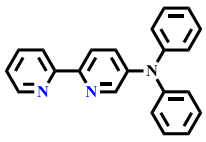

2: A mixture of 5−bromo−2,2′−bipyridine (**a**) (940 mg, 4.0 mmol) and diphenylamine (811.2 mg, 4.8 mmol) was dissolved in toluene (40 mL). Sodium−*tert*−butoxide (360 mg, 3.6 mmol), tri(dibenzylideneacetone)dipalladium(0) ($Pd_2(dba)_3$, 48 mg, 0.052 mmol), and 2,2′−bis(diphenylphosphino)−1,1′−binaphthyl (BINAP, 68 mg, 0.104 mmol) were added to the solution. The reaction mixture was stirred at 130 °C for 24 h under argon. After cooling to room temperature, the reaction was quenched by the addition of an aqueous solution of EDTA, and the product was extracted with CH_2Cl_2. Crude product was purified by column chromatography on silica gel (hexane / ether acetyl, 10 / 1) to afford light yellow solid of the final product, 800 mg in 62% yield. ^{1}H NMR (400 MHz, $CDCl_3$): 8.64 (d, *J* = 4.8 Hz, 1H), 8.41 (s, 1H), 8.28 (dd, *J* = 7.0, 8.4 Hz, 2H), 7.78 (m, 1H), 7.47 (dd, *J* = 8.7, 2.7 Hz, 1H), 7.31 (m, 4H), 7.10 (m, 7H). ^{13}C NMR (100 MHz, $CDCl_3$): 155.86, 148.94, 146.48, 144.41, 143.36, 136.69, 130.54, 129.52, 129.31, 125.81, 124.66, 123.91, 123.60, 122.78, 121.11,

and 120.29. EI−MS (*m* / *z*): 323.12.

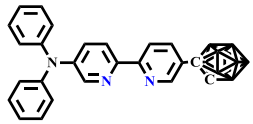

4: 6−bromo−*N*,*N*−diphenylpyridin-3-amine (**b**, 2.53 g, 7.8 mmol) was charged into a flask, kept under vacuum for 20 min, and put under argon. Dry diethyl ether (100 mL) was added from a syringe, and the solution was transferred to a two−neck flask through a cannula. The solution was stirred and cooled to −78 °C. *n*−BuLi (2.4 M in cyclohexane, 3.575 mL, 8.58 mmol) was added dropwise while the color turned from yellow to orange and finally red during the addition. After stirring for 1 h, the reaction mixture turned brown. Trimethylstannyl chloride (1 M in hexane, 10.1 mL, 10.14 mmol) was added dropwise from a syringe, and the solution was allowed to warm to room temperature overnight. Diethyl ether and hexane were evaporated directly from the reaction flask under reduced pressure. Dry hexane (50 mL) was added through a syringe, and the slurry was stirred for 60 min at room temperature. Yellow precipitate was filtered off through a frit under argon, and hexane was evaporated from the filtrate under vacuum, leaving a brown viscous liquid **c** (2.4 g, 75%, 94% purity by ^{1}H NMR). Dry xylene was added, and the crude **c** was used in the next step.

5−*o*−carboranyl−2−bromopyridine (1.0 g, 3.35 mmol) was charged into a flask, evacuated, and put under argon. The crude compound **c** prepared above (2.4 g, 5.85 mmol) in dry xylene (35 mL) was added through a cannula, and argon gas was bubbled through the solution for 2 h. Then, $Pd(PPh_3)_4$ (200 mg, 0.173 mmol) was added from a tip tube. The reaction mixture was stirred at 135 °C for 24 h and subsequently poured into 2 M NaOH (50 mL, saturated with ETDA). Two layers were separated, and the aqueous layer was extracted with diethyl ether (3 × 50 mL). Combined organic layers were dried over Na_2SO_4, and the solvents were evaporated under reduced pressure. The crude product was chromatographed (alumina, 10:1 hexane / ethyl acetate) and **4** was recovered as a yellowish powder: 0.87 g, 65%. ^{1}H NMR ($CDCl_3$): δ 8.73 (d, *J* = 2.1 Hz, 1H), 8.37 (d, *J* = 2.7 Hz, 1H), 8.24 (dd, *J* = 15.2, 8.7 Hz, 2H), 7.84 (dd, *J* = 8.6, 2.6 Hz,

1H), 7.44 (dd, *J* = 8.7, 2.8 Hz, 1H), 7.33 (m, 4H), 7.14 (m, 6H) 3.98 (s, 1H, carborane−CH), 3.20−1.71 (br, 10H, B−H). ^{13}C NMR ($CDCl_3$): δ 157.16, 147.71, 146.72, 146.12, 145.13, 142.72, 135.93, 129.68, 128.21, 128.06, 125.08, 124.44, 121.57, 119.54, 74.01 (carborane−C) and 60.31 (carborane−C). ^{11}B NMR ($CDCl_3$): δ −1.6 (2B), −3.6 (2B), −8.7 (2B), −10.8 (2B), −11.6 (2B). IR (KBr): (ν cm^{-1}) 2588. EI−MS (*m* / *z*): 465.20.

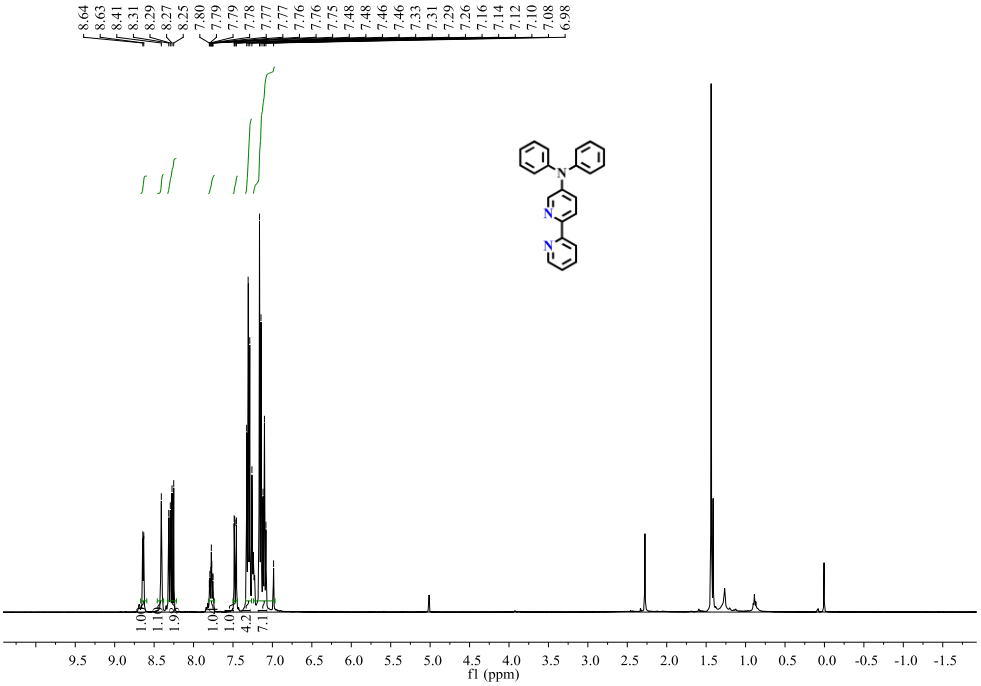

Figure.S1. The ^{1}H−NMR (400 MHz, $CDCl_3$) spectrum of ligand **2**.

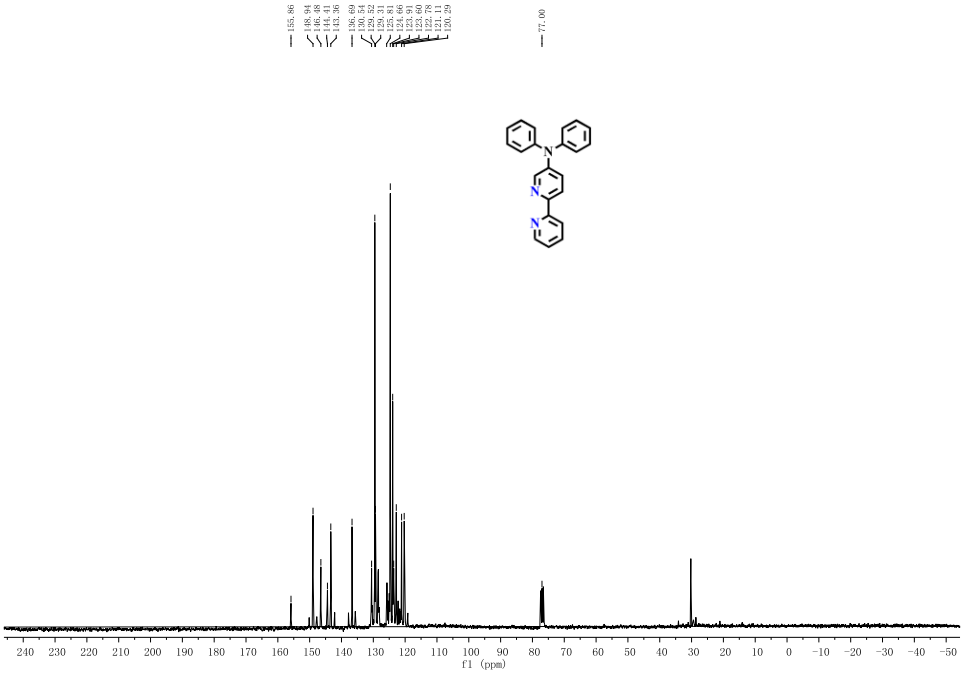

Figure.S2. The ^{13}C−NMR (100 MHz, $CDCl_3$) spectrum of ligand **2**.

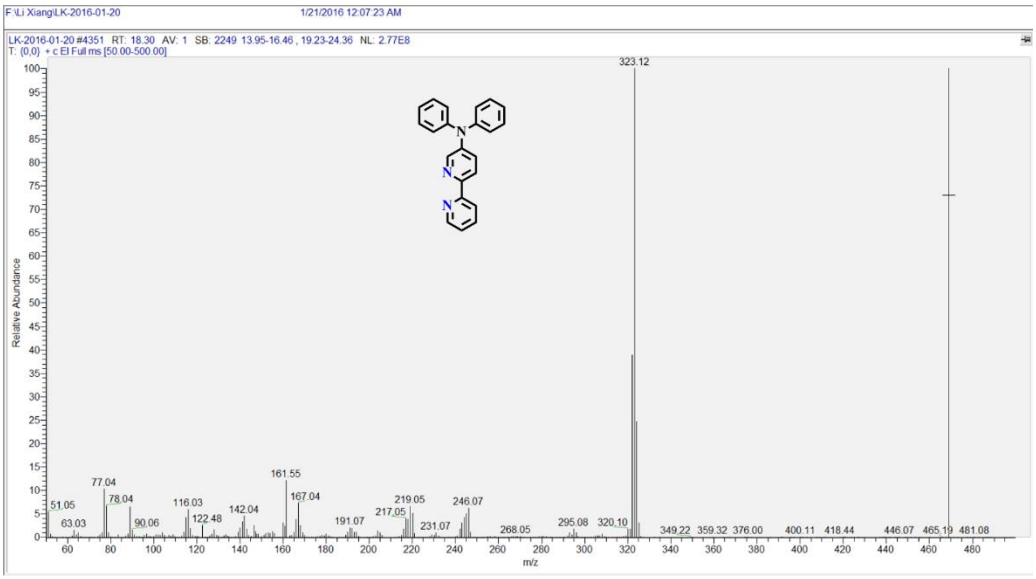

Figure.S3. The EI−MS spectrum of ligand **2**.

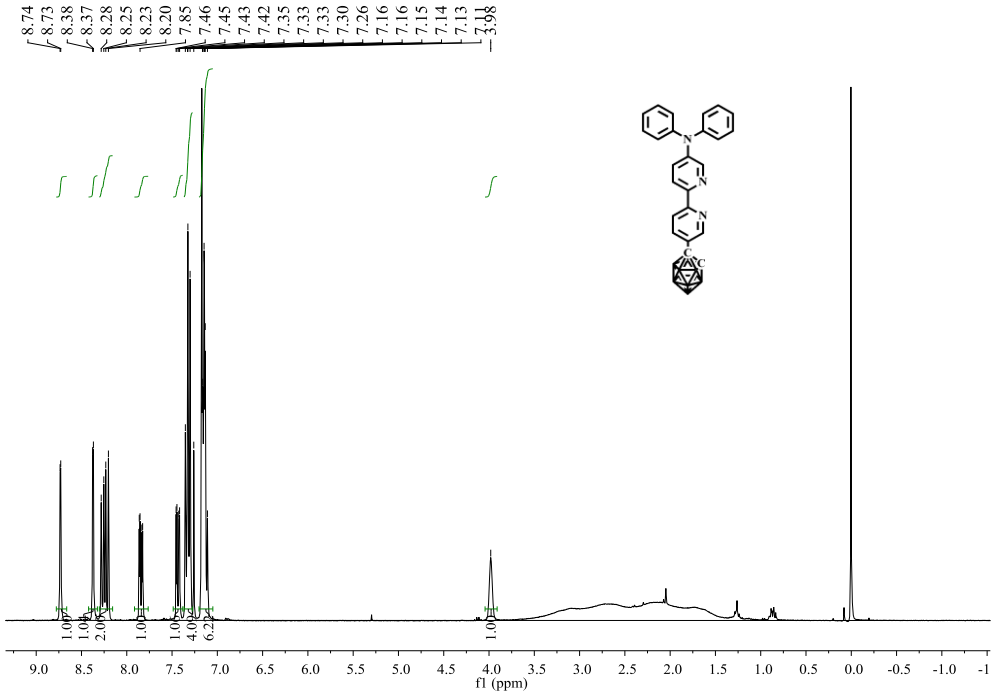

Figure.S4. The ^{1}H−NMR (400 MHz, $CDCl_3$) spectrum of ligand **4**.

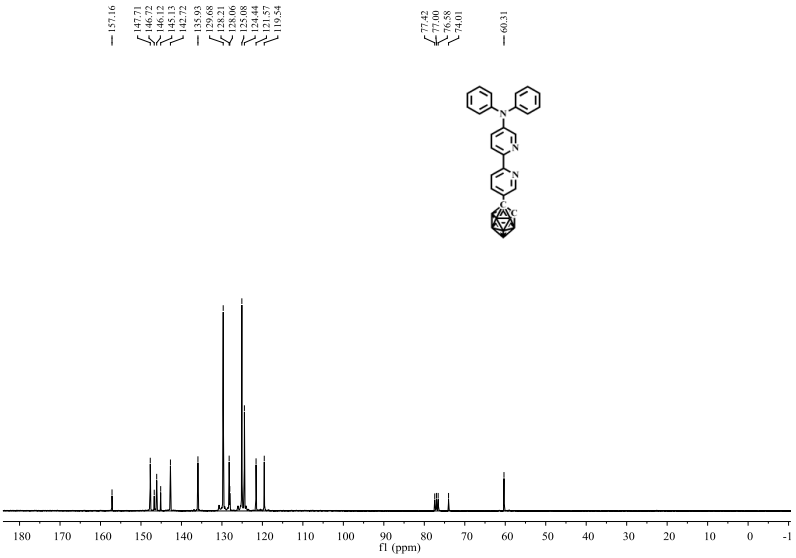

Figure.S5. The $^{13}C-NMR$ (100 MHz, $CDCl_3$) spectrum of ligand **4**.

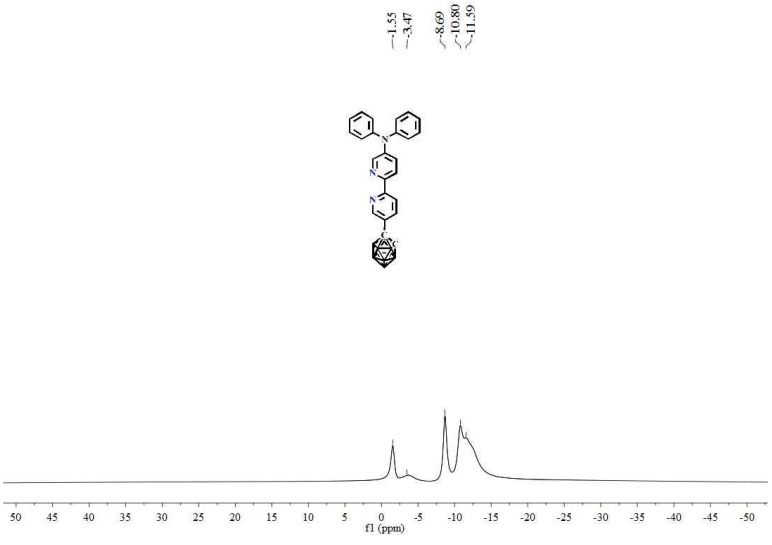

Figure.S6. The $^{11}B-NMR$ ($CDCl_3$) spectrum of ligand **4**.

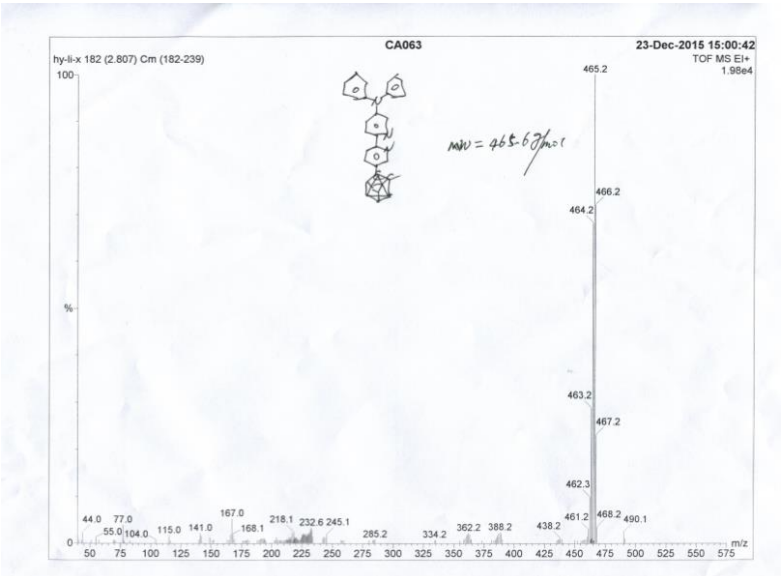

Figure.S7. The EI−MS spectrum of ligand **4**.

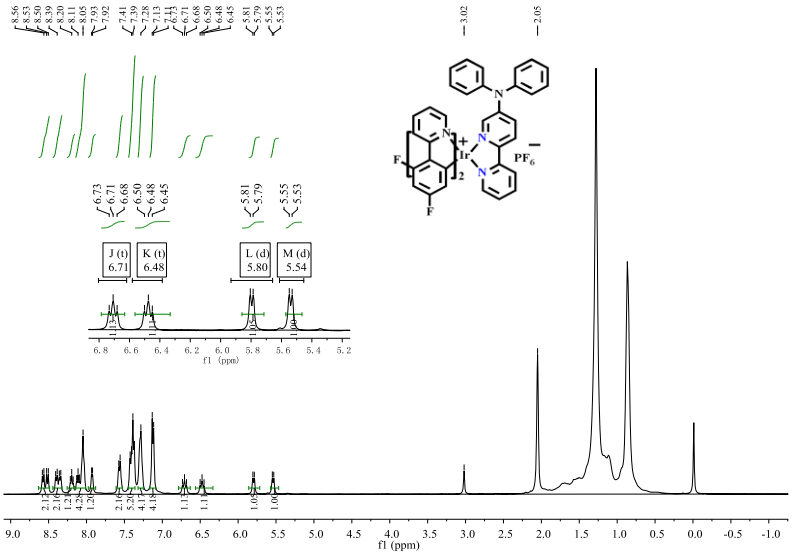

Figure.S8. The ^{1}H−NMR (400 MHz, ^{6}d−acetone) spectrum of iridium complex **II**.

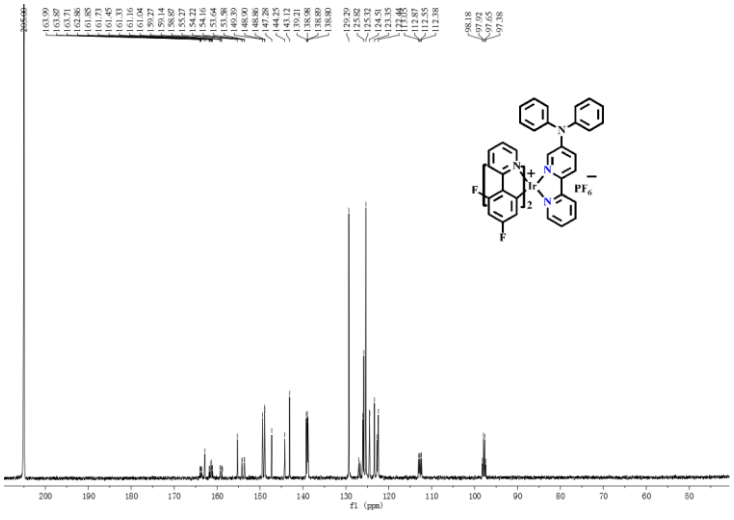

Figure.S9. The ^{13}C−NMR (100 MHz, ^{6}d−acetone) spectrum of iridium complex **II**.

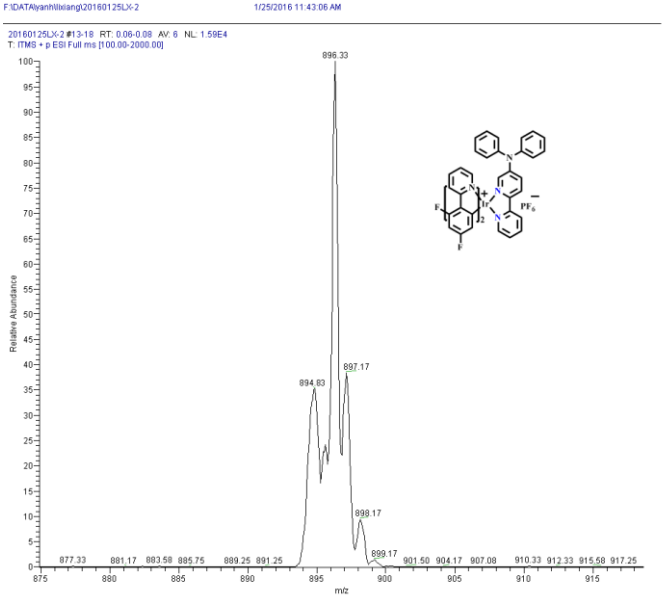

Figure.S10. The ESI−MS spectrum of iridium complex **II**.

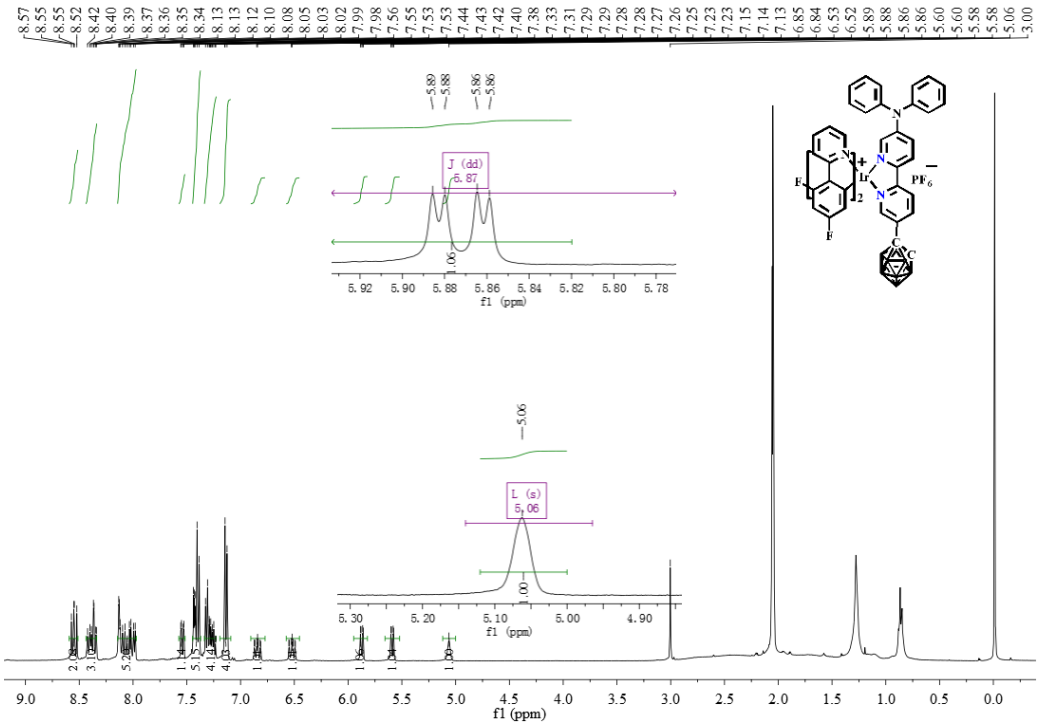

Figure.S11. The ^{1}H−NMR (400 MHz, ^{6}d−acetone) spectrum of iridium complex **IV**.

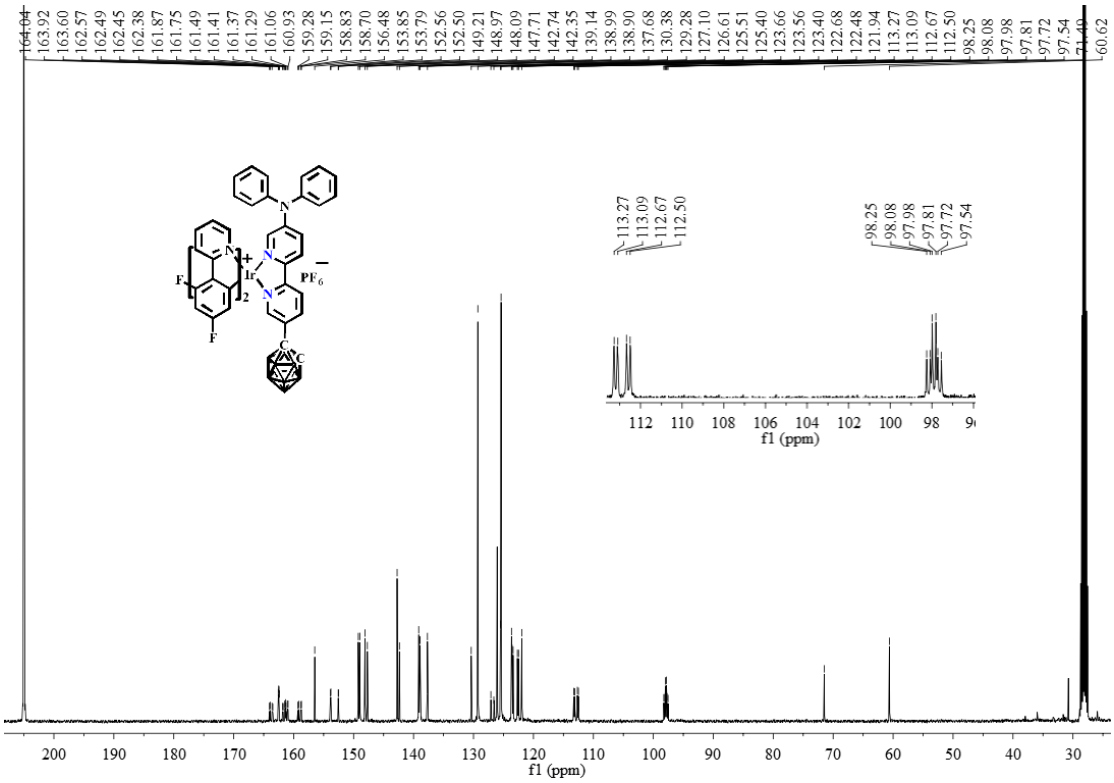

Figure.S12. The ^{13}C−NMR (100 MHz, ^{6}d−acetone) spectrum of iridium complex **IV**.

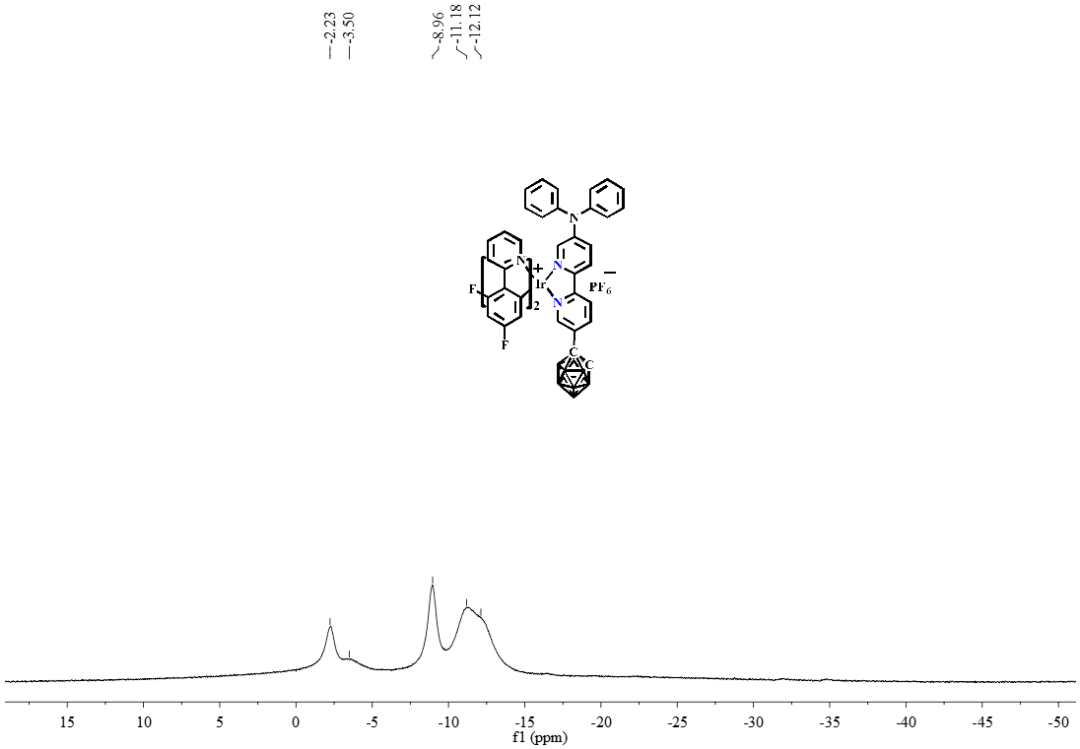

Figure.S13. The ^{11}B−NMR (^{6}d−acetone) spectrum of iridium complex **IV**.

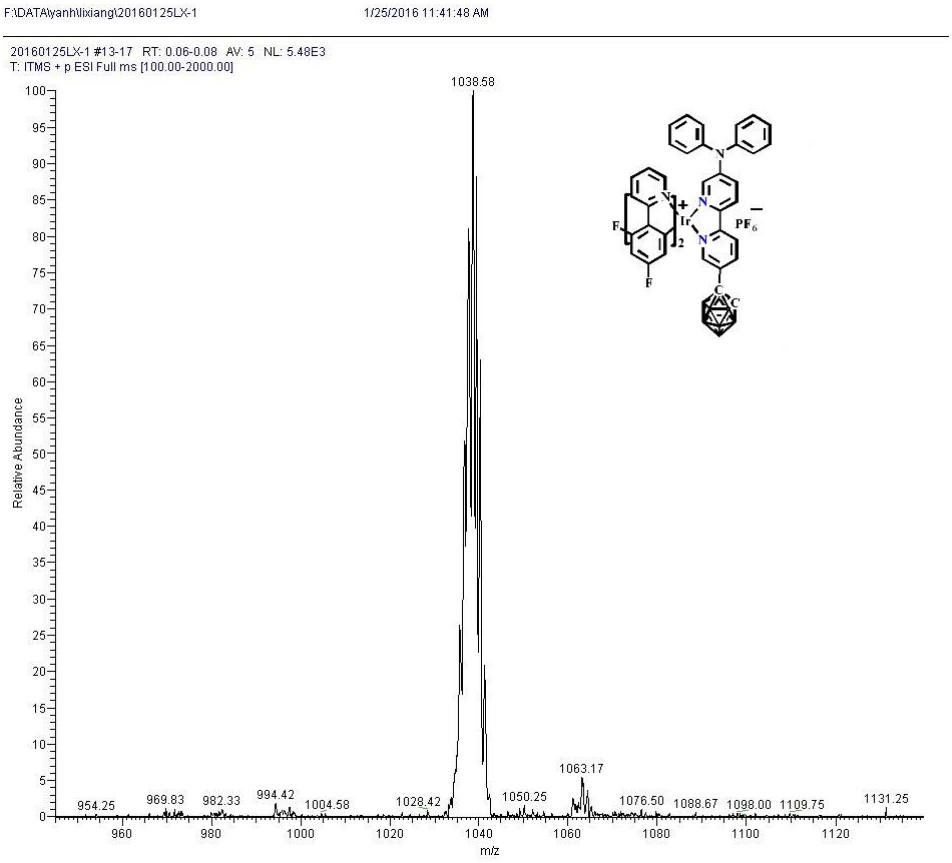

Figure.S14. The ESI−MS spectrum of iridium complex **IV**.

III. X−ray structure determination

The X−ray diffraction data were collected on a Bruker Smart CCD Apex DUO diffractometer with graphite monochromated Mo Kα radiation (λ = 0.71073 Å) using the ω−2θ scan mode. The cell parameters were retrieved using SMART software and refined using *SAINT* for all observed reflections. The data were collected using a narrow-frame method with scan width of 0.3° in ω and an exposure time of 5 s per frame. The redundant data sets were reduced using *SAINT*[6] and corrected for Lorentz and polarization effects. The absorption corrections were applied using *SADABS*.[7] The structure was solved and refined using *SHELXLTL*.[8] Direct method yielded all non-hydrogen atoms, which were refined using anisotropic thermal parameters. All hydrogen atom positions were calculated geometrically and were set riding on their respective atoms. The data were corrected for Lorenz and polarization effects. Structures were solved by direct methods and refined on F^2 by full−matrix least−squares methods using SHELXTL−2016. All calculations and molecular graphics were carried out on a computer using the SHELX−2016 program package and Mercury. CCDC 1564537 (**4**), and 1564536 (**II**) contain the supplementary crystallographic data for this paper. These data can be obtained free of charge from the Cambridge Crystallographic Data Centre via www.ccdc.cam.ac.uk/conts/retrieving.html (or from the Cambridge Crystallographic Data Centre, 12, Union Road, Cambridge CB21EZ, UK; fax: (+44) 1223−336−033; or deposit@ccdc.cam.ac.uk).

Table S1. Crystallographic Data for ligand **4**, and complex **II**.

Compound	**4**	**II**
chemical formula	$C_{24}H_{16}B_{10}N_3$	$C_{44}H_{29}N_5F_4IrPF_6$
formula weight	465.58	1040.89
crystal size (mm)	0.25 × 0.20 × 0.17	0.15 × 0.14 × 0.11
temperature (K)	296(2)	296(2)
radiation	0.71073	0.71073
crystal system	Monoclinic	Monoclinic
space group	P21/c	P2(1)/n
a(Å)	11.738(2)	12.9043(10)
b(Å)	7.3043(14)	25.937(2)
c(Å)	29.418(6)	14.6262(11)
α(°)	90	90
β(°)	94.827(4)	109.2430(10)
γ(°)	90.00	90

V(Å^3)	2513.4(8)	4621.9(6)
Z	4	4
ρ(calc) (g/cm^3)	1.230	1.496
F (000)	968	2040
absorp.coeff. (mm^{-1})	0.065	2.999
θ range (deg)	2.3–26.0	2.0–27.9
reflns collected	14736	32039
indep. reflns	4914	10938
Refns obs. [$I>2\sigma(I)$]	2940	6892
GOF	1.01	1.01
R1/wR2 [$I>2\sigma(I)$]	0.052/0.130	0.040/0.085
R1/wR2 (all data)	0.053/0.1820	0.076/0.1019

IV. Quantum yields determination

Absolute quantum yields of the iridium complexes in all organic solvents and in solid–state were measured by employing an integrating sphere. Lifetime studies were performed with an Edinburgh FL 920 photocounting system with a hydrogen–filled lamp as the excitation source.

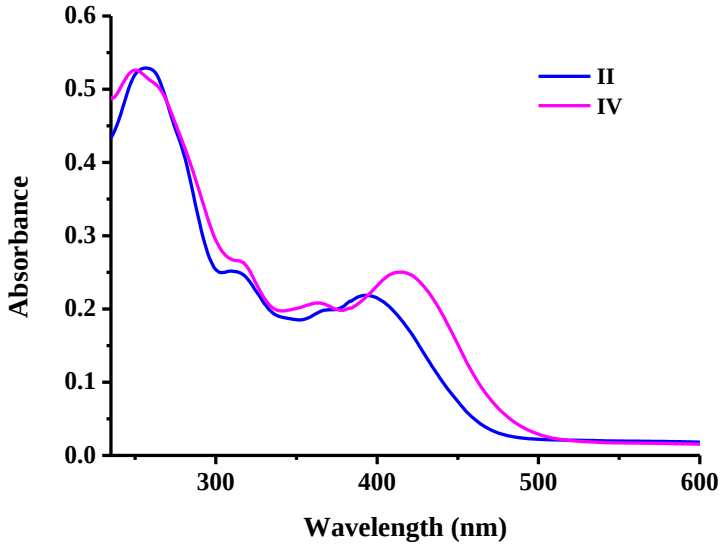

Figure. S15. Absorption spectra of iridium(III) complexes **II** and **IV** in degassed CH_2Cl_2 at room temperature.

Table S2. Absorption spectra data of cationic iridium(III) complexes in degassed CH_2Cl_2 at room temperature.

Complexes	λ_{abs}[a] [nm] (lgε)
I	247(4.0), 303(3.8), 316(3.8), 362(3.1)

II	257(2.5), 313(3.7), 365(3.3), 392(2.5)
III	244(4.0), 296(3.7), 309(3.7), 364(2.9)
IV	248(2.4), 314(3.8), 365(3.3), 415(2.4)
V	249(2.4), 311(3.7), 321(3.8), 364(3.3)

Table S3. Solution emission data of complexes in different degassed solvents at room temperature.

Complexes	**Solvents**	λ_{em} [nm]	Φ_{PL}	τ [ns]
II	toluene	596	0.08	377.3
	CH_2Cl_2	601	0.03	382.3
	$CHCl_3$	601	0.11	406.2
	CH_3CN	601	0.04	289.8
	ethanol	598	0.29	261.5
	DMSO	603	0.14	145.0
IV	toluene	618	0.08	313.1
	CH_2Cl_2	612	0.03	232.2
	$CHCl_3$	612	0.07	257.3
	CH_3CN	608	0.03	117.8
	ethanol	613	0.13	201.2
	DMSO	613	0.10	90.8

V. Quantum chemical calculations

Geometries of all the ligands and iridium(III) complexes were optimized using density functional theory (DFT) method. The electronic transition energies including electron correlation effects were computed by TD−DFT method using B3LYP functional (TD−B3LYP). LANL2DZ basis set was used to treat the heavy metal iridium atom, whilst M06 functional with a basis set of 6−31G (d, p) for C, H, O, N and B atoms. All calculations described here were performed by using Gaussian 09 program.[S6]

VI. Cytotoxicity test

In vitro cytotoxicity was measured using a standard methyl thiazolyl tetrazolium (MTT, Sigma Aldrich) assay in Hela cell lines. Briefly, cells growing in log phase were seeded into 96−well cell culture plate at 1×10^4 / well. Complex **IV** was added to the wells of the treatment group at concentrations of 5, 10, 50, 75 and 100 μmol/L. For the negative

control group, 1 μL / well solvent was diluted in RPMI 1640 with the final concentration of 1%. The cells were incubated for 48 h at 37 ºC under 5% CO_2. Combined MTT / PBS solution was added to each well of the 96−well assay plate and incubated for an additional 4 h. After removal of the culture solution, 200 μL DMSO was added to each well, shaking for 10 min at shaking table. An enzyme−linked immunosorbent assay (ELISA) reader was used to measure the OD570 (absorbance value) of each well referenced at 490 nm. The following formula was used to calculate the viability of cell growth: Viability (%) = (mean of absorbance value of treatment group / mean of absorbance value of control) × 100.

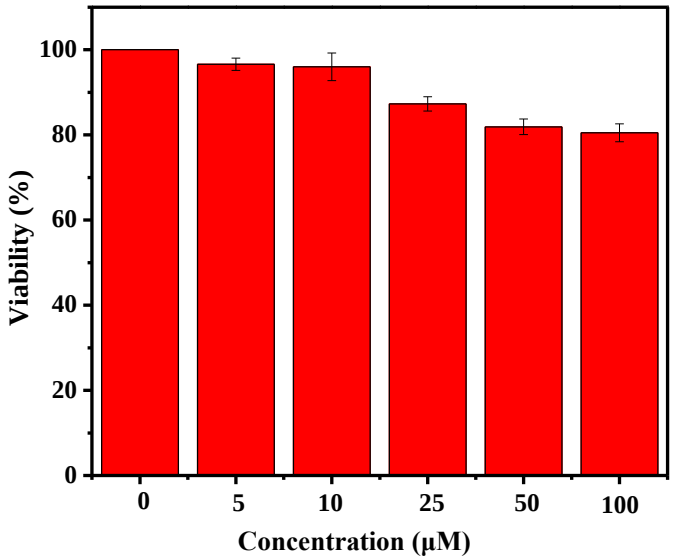

Figure. S16. In vitro viabilities of Hela cells incubated with complex **IV** at different concentrations for 48 h.

VII. Confocal luminescence imaging and phosphorescence lifetime imaging:

Confocal luminescence imaging was carried out on an Olympus IX81 laser scanning confocal microscope equipped with a 40 immersion objective lens. A semiconductor laser was served as excitation at 405 nm. One−photon emission was collected at 450−550 nm for Hela liver cancer cells. For imaging under a certain oxygen concentration, the live cell station equipped with two flow counters which could

respectively control the flow of O_2 and N_2 was used. Complex **IV** was added to RPMI 1640 to yield 10 μM solution, and Hela cells were incubated with the solution of **IV** under 21% or 2.5% O_2 concentrations for 2 hours at 37 °C prior to confocal luminescence imaging.

PLIM image setup is integrated with Olympus IX81 laser scanning confocal microscope. Phosphorescence signal was detected by the system of confocal microscope and correlative calculation of the data was performed by professional software which was provided by PicoQuant company. Light from the pulse diode laser head (PicoQuant, PDL 800−D) with excitation wavelength of 405 nm and frequency of 0.5 MHz was focused on the sample with a 40x / NA 0.95 objective lens for single−photon excitation. The emitted fluorescence signal was collected at 550−650 nm.

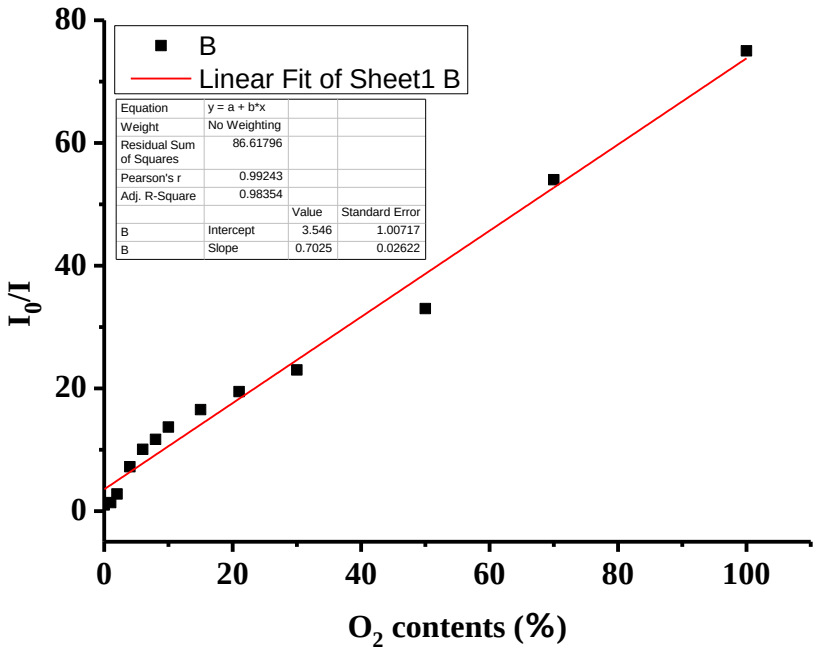

Figure. S17. Plots of R_{I0} / R_I as a function of oxygen pressure.

VIII. References

[S1]: a) S. Lamansky, P. Djurovich, D. Murphy, F. Abdel−Razzaq, H. E. Lee, C. Adachi, P. E. Burrows, S. R. Forrest and M. E. Thompson, *J. Am. Chem. Soc.* **2001**, *123*, 4304−4312. b) C. Liu,

X. Rao, X. Song, J. Qiu and Z. Jin, *Rsc. Adv.* **2013**, *3*, 526−531. c) C. S. K. Mak, D. Pentlehner, M. Stich, O. S. Wolfbeis, W. K. Chan and H. Yersin, *Chem. Mater.* **2009**, *21*, 2173−2175.

[S2]: P. F. H. Schwab, F. Fleischer and J. Michl, *J. Org. Chem.*, **2002**, *67*, 443-449.

[S3]: X. Li, X. Tong, H. Yan, C. Lu, Q. Zhao and W. Huang, *Chem. Eur. J.*, **2016**, *22*, 17282–17290.

[S4]: M.-N. Betzile, X. Wang, Z. M. Hudson and S. Wang, *Dalton Trans.*, **2014**, *43*, 13696–13703.

[S5]: a) M. D. Marshall, R. M. Hunt, G. T. Hefferan, R. M. Adams and J. M. Makhlouf, *J. Am. Chem. Soc.* **1967**, *89*, 3361−3362. b) J. M. Makhlouf, W. V. Hough and G. T. Hefferan, *Inorg. Chem.* **1967**, *6*, 1196−1198. c) I. B. Sivaev, A. V. Prikaznov and D. Naoufal, *Collection. of Czechoslovak. Chem. Commun.* **2010**, *75*, 1149−1199. c) R. N. Grimes, *Carboranes*; 2nd ed., Vol. 9, Academic Press: New York, 2011, pp. 301–540. d) D. Power and T. R. Spalding, *Polyhedron* **1985**, *4*, 1329−1331. e) A. Toppino, A. R. Genady, M. E. El−Zaria, J. Reeve, F. Mostofian, J. Kent and J. F. Valliant, *Inorg. Chem.* **2013**, *52*, 8743−8749. f) L. A. Galliamova, M. V. Varaksin, O. N. Chupakhin, P. A. Slepukhin and V. N. Charushin, *Organometallics* **2015**, *34*, 5285−5290.

[S6]: *SAINT-Plus*, version 6.02, Bruker Analytical X-ray System, Madison, WI, **1999**.

[S7]: G. M. Sheldrick, SADABS - *An empirical absorption correction program*; Bruker Analytical X-ray Systems, Madison, WI, **1996**.

[S8]: *SHELXTL refinement program version 2016/6*: G. M. Sheldrick, *Acta Crystallogr., Sect. C: Cryst. Struct. Commun.* **2015**, *71*, 3-8.